

## **SURFACE MORPHOLOGY OF A MICROPLASTIC AS AN INDICATOR OF ITS MICROSCALE DEGRADATION**

Kamil A. MAJEWSKI<sup>1</sup>, Sylwia MYSZOGRAJ<sup>2</sup>,  
Ewelina PŁUCIENNIK-KOROPCZUK<sup>2</sup>

<sup>1</sup>The Science and Technology Park of the University of Zielona Góra, Poland

<sup>2</sup>University of Zielona Góra, Zielona Góra, Poland

### **A b s t r a c t**

Most of the plastic produced, being one-use plastic packaging, is finally disposed of into the environment. Several agents such as solar radiation, mechanical forces, and microbial action may enable the degradation of these plastics. The purpose of this article is to present a method for studying the properties of a surface of a microplastic particle affected by erosion at the microscale level, which occurred with the help of destructive forces associated with the impact of the sea. The results of analysis of the morphology of the tested sample of microplastic (consisting of poly(propylene)) allowed observing how it was degraded. Examining the surface of a microplastic, one can analyze a number of factors as well as determine the possible path the material has traveled until it was collected as a sample. By determining the scale of the patterns, it is possible to estimate how long the sample and other microplastics present in marine environments have been there. The use of an Atomic Force Microscope not only allows the surface of the sample to be imaged in a non-destructive manner but also enables the degree of degradation to be calculated mathematically, provided a baseline is established from which erosion can be assumed to have originated.

**Keywords:** microplastic, degradation, poly(propylene), analytical methods

---

<sup>1</sup> Corresponding author: The Science and Technology Park of the University of Zielona Góra, Poland, e-mail: k.majewski @pnt.uz.zgora.pl

## 1. INTRODUCTION

The use of plastics has significantly improved the quality of human life [1]. Through their daily use in both industry and households, plastics can be considered a pillar material in a global economy based on a “throwaway culture”. Plastics have made it possible to use more economical, lightweight products and to produce materials with properties required for a wide range of human needs [2]. Versatile, durable, and with great potential for adaptation to different needs, plastics are a group of extraordinary materials, inextricably linked with innovation and science. Global plastic production has been steadily increasing and in 2019 amounted to 386 million tons (51% from Asia, of which 31% China, 5% Japan, and 17% the rest of Asia), and in Europe, 58 million tons (16%). In Europe in 2019 most plastics were intended for packaging (39.6%), building and construction (20.4%), and the automotive industry (9.6%). Plastic demand distribution by resin type was as follows: poly(propylene) (PP) (19.4%), PE-LD/PE-LLD (17.4%), PE-HD/PE-MD (12.4%), other thermoplastics (11.3%), PVC (10%), PUR (7.9%), PET (7.9%), other plastics (7.5%), and PS+EPS (6.2%). Now, and in the future, plastics will still be in use, however, it is necessary to take global measures to reduce the amount of plastic waste discharged into the natural environment and its corresponding negative impact. Currently, most plastics are produced on the basis of fossil raw materials: crude oil or natural gas, while in the future most plastics will be produced on the basis of such raw materials as, e.g., used oils, plastic waste, biomass obtained in accordance with the principles of sustainable development, or even CO<sub>2</sub> [3].

A significant problem, widely reported in the literature, is the presence of plastics, and especially microplastics (MPs), in the environment. It is estimated that by 2050, the accumulation of individual plastic waste in the environment will reach about 12 billion tons, according to the current volume of plastics output and waste management [4]. Plastics are intentionally as well as accidentally deposited into the environment, even in remote locations such as Antarctica [5], mountain tops [6], and ocean depths (where they become available as food for a wide range of organisms incidentally interested in them, such as zooplankton, clams, shrimp, fish, or whales) [7]. MPs are synthetic polymers of petrochemical origin, practically insoluble in water, and non-biodegradable solids in the form of fibers, ellipsoids, granules, shot, and flakes. MPs are said to be particles with diameters of between 1 μm and 5 mm. They can be classified into small MPs (<1 mm) and large MPs (1–5 mm) [8]. Classifying MPs as particles with diameters <1 mm is more logical because ‘micro’ generally refers to a micrometer size range [9]. The sources of MPs are various, most commonly residential households, landfills, construction, factories, farmland, ships, and marine platforms [10]. MPs are further classified as primary and secondary. Primary MPs are plastic particles that

are produced in the form of microscopic particles and are a by-product of washing synthetic clothes (35%), abrasion of tires (28%), or smog (24%) that are released directly into the environment. Secondary MPs are formed during the use or decay of plastic products. The main source of secondary MPs is waste, which comes from a wide range of products, often of large dimensions, and explains why they are so common in wastewater, waste, and the environment. Secondary MPs make up 69-81% of the MPs floating in the seas and oceans (e.g., plastic bags, fishing nets) [11].

Many analytical techniques are available to characterize MPs. Procedures typically include separation, identification, and quantification and most use analytical techniques to identify and/or quantify microplastic which are based on spectrometry, microscopy, and/or thermal analysis. To identify the type of plastic, various types of spectroscopy are used such as Raman spectroscopy (2 mm), time-gated Raman method spectroscopy ( $\leq 125$  mm and  $\geq 5$  mass %), Micro-Raman spectroscopy ( $> 100$  mm), Micro-FTIR spectroscopy ( $> 100$  mm), m-Raman spectroscopy ( $> 1$  mm), m-FTIR spectroscopy ( $> 10$  mm), macroscopic dimensioned near-infrared (NIR) in combination with chemometrics ( $> 10$  mm and 1 mass%) and hyperspectral imaging technology (0.5-5 mm) [10]. To simultaneously identify polymer types of MP particles and associated organic plastics, additives are used to obtain a precise MP weight, for example, sequential pyrolysis-gas chromatography coupled with mass spectrometry (PY-GC-MS) and thermal extraction desorption gas chromatography mass spectrometry (TED-GC-MS) [12].

The content of copolymers and additives with different photooxidation and biodegradation routes makes the identification of MPs very limited [13]. It is reported that on the basis of visual observation, approximately 20% of the particles initially considered to be MPs are later determined by scanning electron microscopy (SEM) as aluminum silicate from carbon ash [14]. Other sources indicate that 32% of particles smaller than 100 mm that were visually counted as MPs were not confirmed by micro-Raman measurements [14,15].

Every MP in the environment is degraded. It should be noted that plastics are generally resistant to decomposition, and the period of complete degradation of plastic waste in the environment ranges from decades to centuries [16]. The decomposition process is the result of chemical changes in the polymer structure that reduce its molecular weight, which weakens the material's mechanical integrity [17]. In the literature, there are works describing the environmental biodegradation of microplastics: theoretical works [18, 19], research using simulated conditions [14, 20, 21], and studies of the environmental effects [22,23].

The purpose of this article is to present a method for studying the properties of the surface, at the microscale level, of an MP particle affected by erosion, which

occurred with the help of destructive forces associated with the impact of the sea. The surface is a three-dimensional region extending around some mathematical two-dimensional surface, which affects the described phenomena at a given location [24].

## **2. MATERIALS AND METHODS**

### **2.1. Materials**

MP sampling methodologies can be specified for bulk and reduced volume sampling [25]. For the purpose of this study, the sample was collected using a manual method; by sampling onshore, in the scour zone, where MPs tend to accumulate most under wave action [26]. No selective, volume-reduced, or bulk sampling strategy was used [25] because the study is intended to illustrate how the environment affects the particle surface of a given MP sample. Approximately 20 samples of MP particles were collected, but only one was selected for AFM because of its ability to be placed in the measuring apparatus. Material was collected during fieldwork performed on May 3, 2021.

The material collected during fieldwork was used to conduct a study of the morphology of the microplastic surface. The chosen location for sampling was the coastal area of the Baltic Sea in north-western Poland, in the northern part of the West Pomeranian Province, in the Kolobrzeg district. The exact GPS location is 54°11'23.7"N 15°36'14.8"E. The fragment of MP collected was originally submerged in seawater and then dumped on land being part of the sandy beach.

### **2.2. Preparation of the sample**

Due to the nature of the study as well as the laboratory analysis, the sample preparation procedure was different from that suggested in the Guidelines for sampling microplastics on sandy beaches [27]. The sample was collected directly into a plastic container due to its greater flexibility, which, in the event of shock during handling, minimized the possibility of artificial deformation. In the laboratory, the sample was cleaned with a blast of warm air from a Reeco RA-150, and a Nikon SMZ745T stereo microscope was used to check that the surface of the sample was made of homogeneous material and that no sand grains were knocked in. Brush cleaning of the specimen couldnot be performed due to the possibility of disturbing the test results by scratching the specimen surface. The sample, after removing adhered sand particles, was divided into two parts. The first part was used for qualitative analysis, which was performed by FTIR – ATR and Raman techniques, while the second part became the main element to perform a microscale surface morphology study. To prepare the sample fragment for quantification by FTIR – ATR analysis, it was placed in a press (Specac, SN:

P32251) with a pressure of 2 tons to obtain uniform contact between the solid sample and the diamond ATR crystal. The sample was then tested for quantification. After obtaining the results from the Fourier transform infrared spectroscopy (FTIR) analysis, the sample so prepared was transferred to a basic microscope slide for further verification analysis by Raman spectrum. The second part, left for the actual study of surface morphology by Atomic Force Microscope (AFM) microscopy, was transferred unaltered and immobilized with double-sided adhesive tape in a basic microscope slide.

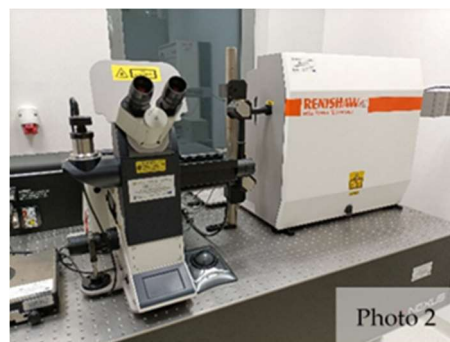
### 2.3. Apparatus and software

The following apparatus and software were used to perform qualitative analyses of the sample:

- Nicolet™ iS50 FTIR spectrometer with ATR attachment from Thermo Scientific™, SN: AUP1400379, with dedicated OMNIC 9.2.106 software (driver version: 9.2, firmware version: 1.11), which is part of the equipment at the Science and Technology Park of the University of Zielona Góra Ltd (Photo. 1). Fourier transform infrared spectroscopy (FTIR) is an analytical technique used to understand the structure of single molecules and the composition of molecular mixtures. FTIR spectrometers allow absorption to be monitored, and because each molecule vibrates slightly differently, a unique infrared spectrum can be obtained [28, 29].



- Renishaw's Raman inVia™, SN: 168J35, confocal microscope with software: wire 3.4 HF6488. HF6657, build 2377, which is part of the equipment of the Science and Technology Park of the University of Zielona Góra Ltd. Spectrum matching using: database Renishaw polymeric materials (Photo 2). Raman spectroscopy belongs to the category of vibrational spectroscopy [30], meaning that it analyzes a sample chemically by using light (nowadays, mainly laser is used for this purpose) to energetically excite directed particles,



and by using scattered light, the detector is able to interpret this interaction and thus determine what chemical compounds are present in that sample.

- Atomic Force Microscope (AFM) – Bruker’s Bioscope Catalyst EasyAlgin™, SN: 840-006-817 with NanoScope 9.0 software for scanning the sample surface, and NanoScope Analysis 1.5 for processing the images obtained by scanning (which is part of the equipment at the Science and Technology Park of the University of Zielona Góra Ltd.) (Photo 3). The use of weak intermolecular interactions, mainly van der Waals forces, is the basis of AFM imaging. These forces occur between the scanning blade (tip) and the sample surface a short distance away (0.2–10nm) [31]. The AFM technique faithfully reproduces the surface being tested, creating a mathematical three-dimensional image.



#### 2.4. Methods

The artificially unmodified second part of the microplastic sample was used to examine the surface of the test sample. A 500 nm x 500 nm plane was used as the scanning area. To eliminate physical contact in the AFM, which can potentially damage the sample surface, potentially affecting the results and preventing accurate and reliable physical characterization of the sample [32], the ScanAsyst™ method implemented in NanoScope 9.0 software, which is based on Bruker's new general-purpose imaging mode, Peak Force Tapping™, was used to scan the sample. This patented mode performs a very fast force curve on each pixel of the image. The peak force value of each of these curves is then used as the imaging feedback signal. Unlike TappingMode™, in which the imaging force is a complex function of the setpoint and other variables, Peak Force Tapping mode provides direct force control. This allows operation at even lower forces than in TappingMode, which helps protect delicate samples and tips [33]. The result is a spatially dimensioned image.

### 3. RESULTS

#### 3.1. Quantification results by FTIR – ATR spectroscopy

It is accepted that for quantification results using FTIR to be considered adequate, the fit factor should be above 90%. Peak heights for wavelengths 2800-3000 and 800-1600 of the test sample were analyzed with the Hummel Polymer and Additives FT-IR Spectral Library standard and then an automated comparison of FTIR spectra with polymer databases was used. The best matching coefficient shown by the Thermo Scientific™ Hummel Polymer and Additives FT-IR Spectral Library database (which is one of the most comprehensive and widely used libraries for polymer material analysis [34]) was 85.42, classifying the sample as poly(propylene) (PP). A match rate below 90% may be due to the origin of the material, which was picked up from the sea where impurities may have accumulated on its surface, so it was decided to subject the sample to a more thorough investigation using Raman spectroscopy. The results of the FTIR - ATR spectrum for the MP particle and the results of fitting the obtained spectrum to databases are presented in Figure 1.

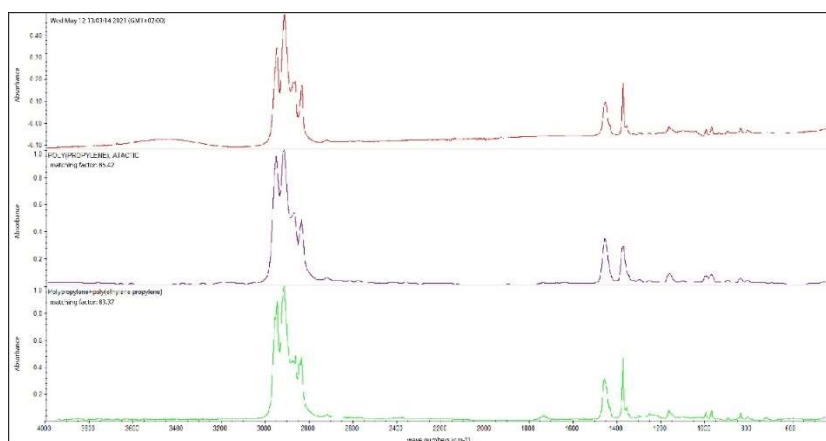


Fig. 1. FTIR – ATR spectrum results for the MP particle under study and results of matching the obtained spectrum with the databases

PP has a density of  $9,000 \text{ kg/m}^3$  and is the lightest material. The market share of the PP homopolymer (PPH) is 65-75%. It is not possible to use PP at temperatures below  $0 \text{ }^\circ\text{C}$ , but it has excellent resistance to diluted and concentrated acids, alcohols, and bases, good resistance to aldehydes, esters, aliphatic hydrocarbons, ketones, and limited resistance to aromatic and halogenated hydrocarbons and oxidants [35]. The crystal structure of PP gives it a high level of stiffness and is responsible for a high melting point compared to other thermoplastics [18, 35]. Environmental weathering is a slow process and causes decomposition

of plastics and changes in the properties of polymers. Degradation occurs as a result of biological and / or abiotic processes such as light, temperature, air, water, and mechanical forces [12]. Mechanical degradation is the breakdown of plastics as a result of external forces such as the impact and abrasion against rocks and sand caused by wind and waves. Biological degradation, on the other hand, is caused by microorganisms. The oxidation and chain scission of polymers are caused by degradation, leading to changes in the chemical composition, texture, physicochemical properties, and mechanical properties of the plastics. That is why the changes in those properties can be used to characterize the degree of plastic degradation [12,36].

### 3.2. Quantification results using the Raman spectrum

Vibrational spectroscopic methods (FTIR or Raman spectroscopy) are the most common methods for the identification and quantification of MPs because of the availability of multi-analysis. Characterization based on the polymeric chemical structure and identification by comparison with known reference spectra is possible [37].

The Renishaw confocal Raman in Via™ microscope was used to check the nanoscale uniformity of the sample. By inspecting several optically distinct points, identical spectra were obtained, allowing the sample to be classified as a single material (Figure 2). The resulting spectra and a match to the database Renishaw polymeric materials are shown in Figure 3. Matching the database with the obtained spectrum indicates, as before with Fourier analysis of the sample, the sample is poly(propylene).

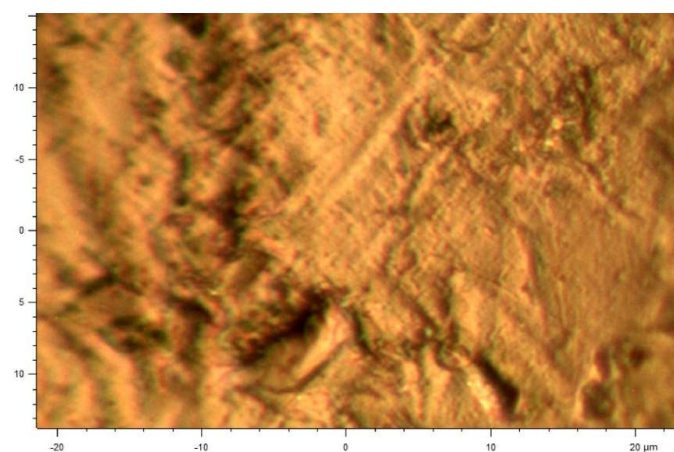


Fig. 2. Three points were used to make Raman spectra at an optical magnification of x50. The image shows the area that was used to make the spectra



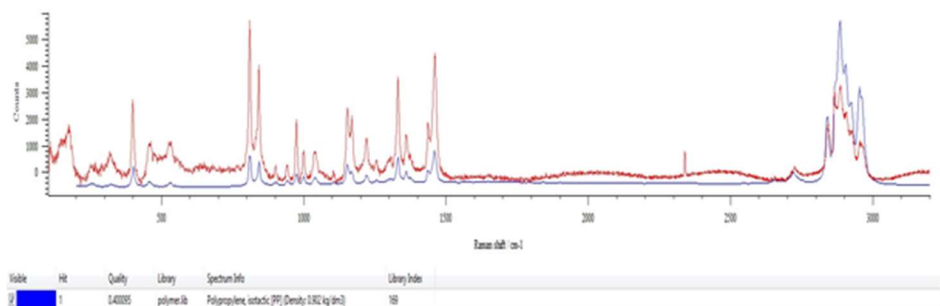


Fig. 3. Raman spectrum of the sample (red) and the level of matching in the database Renishaw polymeric materials

Analysis of the position of the peaks in the  $400\text{--}1500\text{ cm}^{-1}$  wavelength range clearly shows similarity to the reference sample. The  $2300\text{--}2400\text{ cm}^{-1}$  peak was considered to be an artifact, while the automatic matching of the spectrum to the base in the software is without question (98% of Polypropylene). Reference sample information: Polypropylene, isotactic [PP] (Density:  $0,902\text{ kg/dm}^3$ ), Molecular formula  $[-\text{CH}_2\text{CH}(\text{CH}_3)-]_n$ . Experimental parameters: Excitation wavelength:  $514\text{ nm}$ , Exposure time:  $10\text{ s}$ , Laser power on sample:  $4,2\text{ mW}$ , Objective  $\times 50$  Leica N Plan.

### 3.3. Result of surface scanning with Bruker AFM (Atomic Force Microscope)

The main state of the plane is shown in Figure 4, where the heights of the different parts of the scan area are color-coded. Data on the total height difference in the scanned area of the sample are included in Figure 5.

Setting parameters for conducting the experiment: Scan Size –  $500\text{ nm}$ , Scan Rate –  $0.501\text{ Hz}$ , Samples/Line –  $256$ , Lines –  $256$ , Line Direction – Retrace, Data Type – Height, Scan Line – Main, Date –  $02:03:07\text{ PM Wed May 19, 2021}$ , Tip Model – NTESP, Tip Part – MMP-11200-10, Tip Manufacturer – Veeco, 3601 Cale Tecate Suite C, Camarillo, CA 93012, Aspect Ratio –  $1.00$ , Capture Direction – Up, Amplitude Setpoint –  $250.00\text{ mV}$ , Drive Amplitude –  $32.96\text{ mV}$ . Scan area result parameters: Box Area –  $250000\text{ nm}^2$ , Centre Line Average –  $1147.94\text{ nm}$ , Bearing Area –  $250000\text{ nm}^2$ , Bearing Area Percent –  $100.000\%$ , Bearing Depth –  $630.629\text{ nm}$ , Bearing Volume –  $287579968\text{ nm}^3$ , Histogram Area –  $3471.37\text{ nm}^2$ , Histogram Percent –  $1.3885\%$ , Histogram Depth –  $1131.95\text{ nm}$ .

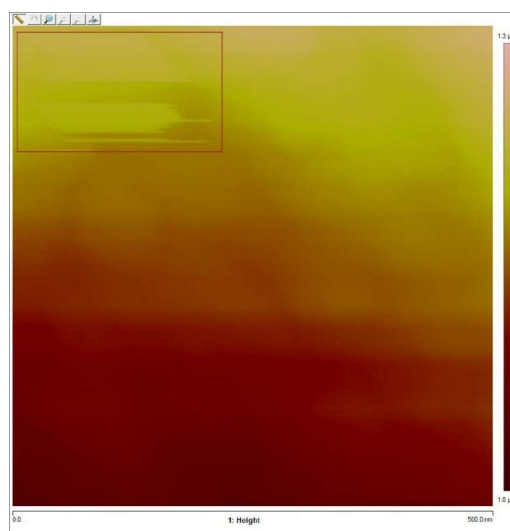


Fig. 4. Result of surface scanning with AFM by ScanAsyst. 2D view showing where the sample was shielded from the erosion process

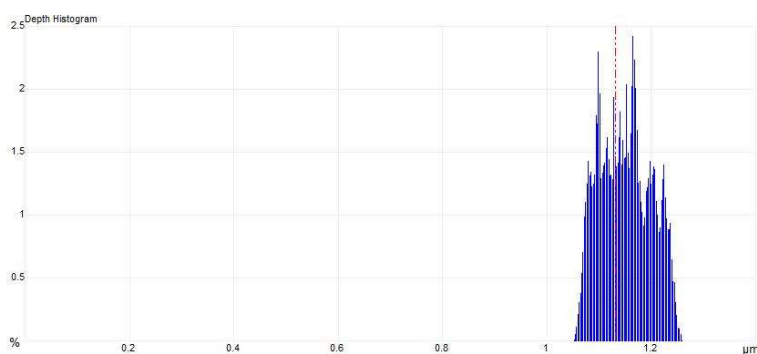
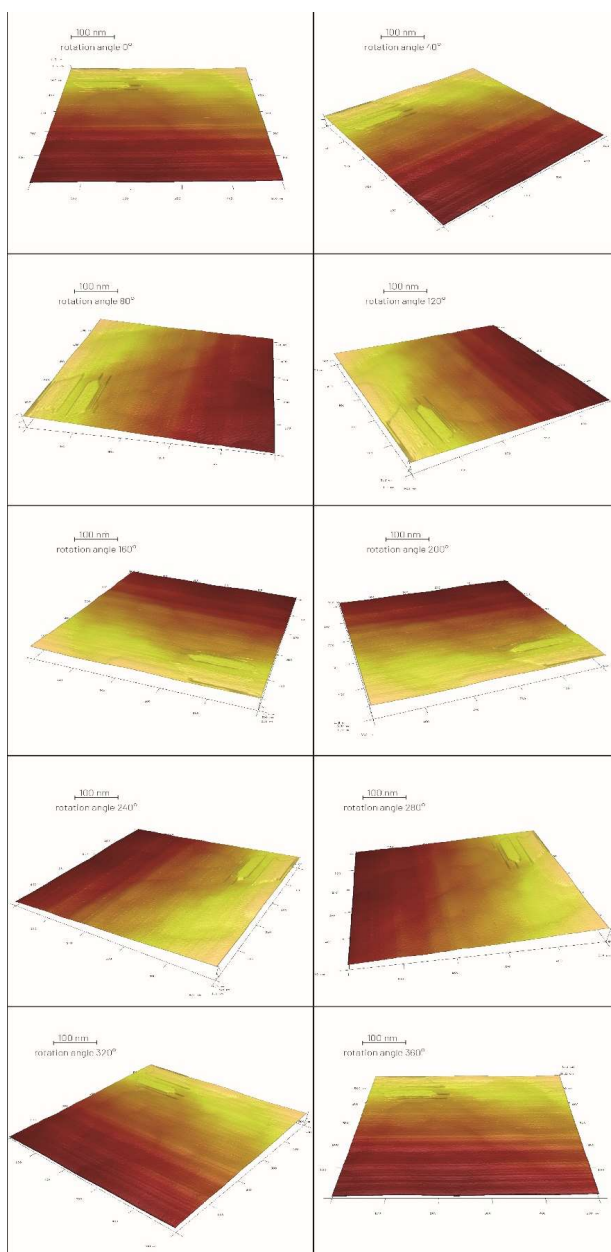


Fig. 5. Graphical representation of height differences in the studied sample

In Table 1 the surfaces of the scanned area can be seen in the 3D plane at different angles. In order to obtain a suitable image for 3D analysis, the tilt of the study area was set to  $50^\circ$  and images with a rotation of  $40^\circ$  were exported from the program. Parameters common to all images - Projection: Perspective; Plot Type: Mixed; Skin Type: Ch 1; Pitch:  $50.0^\circ$ ; Light Rotation:  $0.00^\circ$ ; Light Pitch:  $90.0^\circ$ ; Light Intensity: 49.0 %; Specular light: 37.0 %; Specular reflection: 98.6 %; Specular exponent: 20; Label Type: All; Background Color: White; Zoom: 1.25; xTranslate: -13.9; yTranslate: 2.72; Z-axis Aspect Ratio: 0.100.

Table 1. View of the image sequence of the scanned area in the 3D plane



In Table 2, the values of measurement parameters analysis with the use of NanoScope Analysis 1.5 software are included.

Table 2. Summary of calculated results from NanoScope Analysis 1.5 software

Results*	
Image Raw Mean	1150 nm
Image Mean	1150 nm
Image Z Range	207 nm
Image Surface Area	298217 nm <sup>2</sup>
Image Projected Surface Area	250000 nm <sup>2</sup>
Image Surface Area Difference	19.3 %
Image Rq	7.65 nm
Image Ra	6.17 nm
Image Rmax	44.4 nm

\* Image Raw Mean - Mean value of data contained within the whole image, except for stop bands. This is calculated as if the OL Plane fit were set to None during image capture. Image Mean - Mean value of data contained within the whole image, except for stop bands. This is calculated after the OL Plane fit set during image capture has been applied. Image Z Range - Maximum vertical distance between the highest and lowest data points in the image prior to the planefit. Image Surface Area - The three-dimensional area of the entire image. This value is the sum of the area of all of the triangles formed by three adjacent data points. Image Projected Surface Area - Area of the image rectangle (X x Y). Image Surface Area Difference - Difference between the image's three-dimensional surface area and two-dimensional projected surface area. Image Rq - Root mean square average of height deviations taken from the mean image data plane. Image Ra - Arithmetic average of the absolute values of the surface height deviations measured from the mean plane [38]. Image Rmax - Maximum vertical distance between the highest and lowest data points in the image following the planefit.

The erosion of the tested MP sample can be analyzed based on the use of the term "erosive wear", that is, the operation of mechanisms that affect the wear process when erosive particles hit the surfaces of mechanical components [39]. Deformation of the surface of the tested material began with the formation of shallow indentations, which is visible on most of the surface of the tested sample. Also on this surface, it can be assumed that the erosion was caused by impact or so-called impact erosion, which is a process of gradual loss of material from the surface due to repeated and repeated impacts of abrasive particles contained in the gas stream [40]. The same surface has also been subjected to impact erosion by the action of a liquid as can be seen by the pitting, dulling of the surface. The surface of the material due to the impact of the abrasive particles is strengthened by crushing. The strengthened subsurface layer acts as a barrier and triggers the wear mechanism, which is fatigue of the surface layer.

Another example of erosion observed in the MP sample studied is that caused by abrasion, due to low angle impact of abrasive particles with sharp edges, which are up to four times more effective in removing material from the eroded surface compared to spherical particles and tend to reduce the effect of particle interference [41]. With the AFM technique, this can be accurately observed in the marked section in Figure 4. In the case of erosion action caused by abrasion, it can be assumed that there was a loss of mass of the material and detachment of a smaller piece of MP thus creating another MP particle.

Continued advances in the chemical and physical characterization of MPs are important for a more accurate and thorough understanding of their impact on the environment. We know that MPs are found throughout the environment, we now need to better understand in what form and how they interact. The physical properties of plastic microparticles can affect their reactivity and thus their behavior in the environment [42]. Therefore, studying the relationship between physical characteristics (such as surface roughness) and the sorption behavior of different polymers is important for understanding the behavior of MPs. As suggested by S. D. Burrows, S. Frustaci, K. V. Thomas, and T. Galloway, AFM techniques can be applied to the study of microplastics for sorption studies, UV degradation, and surface roughness characterization. This would facilitate a more in-depth study of the relationship between physical properties and sorption and help expand microplastic characterization in the literature [43].

A technique for studying the surface of microplastics has also been applied by S. Selvam, A. Manisha, S. Venkatramanan, et al., in their work: Microplastic presence in commercial marine sea salts: A baseline study along Tuticorin Coastal salt pan stations [44]. Nevertheless, their AFM study was only to show the differences in surface degradation for four polymers. Analysis of the surface morphology of the tested sample of MP (consisting of polypropylene) allowed observation of how it was degraded, showing obvious signs of roughness such as surface irregularities not resulting from its shape [45]. In the case of the test sample, there is a clear area that was shielded from erosion as indicated in Figure 4, while the entire remaining surface was slowly degrading. In the case of the polypropylene MP sample, it can be assumed that the roughness is due to mechanical and chemical weathering associated with the activity of marine processes. The only exception that would suggest a high destructive force is the fragment seen at Y: 300-500 nm, X: 0-200 nm. This is the highest Z-axis portion of the microplastic examined. It would need further investigation to establish whether this is the result of destructive force or whether this fragment was shielded by another material with different properties that protected the surface beneath it, and then further erosion occurred after degradation of that material.

### 3. CONCLUSIONS

FTIR and Raman spectra are commonly used for characterizing the chemical changes of plastics during the degradation and identification of microplastics. The use of AFM not only allows the surface of the sample to be imaged in a non-destructive manner, but also the degree of degradation to be calculated mathematically, provided a baseline is established from which erosion can be assumed to have originated.

When testing a sample that we know nothing about except for its quantification in terms of the type of material it is made of, we can only guess how to establish a baseline to calculate the amount of material that has eroded. Very useful in this study is the fact that the AFM gives direct information about the value of the vertical displacement of the probe blade, and more importantly, gives the result of the measured actual surface in relation to the planned surface.

In the case of the test sample, the planned measured area was 250000 nm<sup>2</sup>, while the value measured by AFM was 298217 nm<sup>2</sup>. This is a difference of 19.3% from the planned area to the imaged area (data directly from NanoScope Analysis 1.5 software).

The situation would be different if we could identify which product a given microplastic fragment came from. In that case, one could try to use comparative analysis and thus determine a more accurate baseline and the amount of material that has been eroded by various environmental factors.

The conclusions of the analysis are an excellent contribution to further research using AFM in the study of microplastics. Using the AFM technique, one is tempted to suggest that it is also possible to answer the question of what size particles have been detached and whether they are still further microplastic particles.

**REFERENCES**

1. Galloway, TS 2015. *Micro- and Nano-plastics and Human Health. Marine Anthropogenic Litter*. Bergmann, M, Gutow, L, Klages, M. (eds). Springer, Cham. 343, [https://doi.org/10.1007/978-3-319-16510-3\\_13](https://doi.org/10.1007/978-3-319-16510-3_13).
2. Oliveira, M and Almeida, M 2019. The why and how of micro(nano)plastic research. *TrAC Trends in Analytical Chemistry*, **114**, 196-201, <https://doi.org/10.1016/j.trac.2019.02.023>.
3. Plastics – the Facts 2020 An analysis of European plastics production, demand and waste data. Available online: <https://www.plasticseurope.org/en/resources/publications/4312-plastics-facts-2020>, (accessed on: 25-07-2021).
4. Geyer, R, Jambeck, JR, and Law, KL 2017. Production, use, and fate of all plastics ever made. *Sci. Adv.* **3**, 25–29, doi:10.1126/sciadv.1700782.
5. Waller, CL et al 2017. Microplastics in the Antarctic marine system: An emerging area of research. *Science of The Total Environment* **598**, 220-227, doi: <https://doi.org/10.1016/j.scitotenv.2017.03.283>.
6. Free, CM, Jensen, OP, Mason, SA, Eriksen, M, Williamson, NJ and Boldgiv, B 2014. High-levels of microplastic pollution in a large, remote, mountain lake. *Mar Pollut Bull.* **85(1)**, 156-163, doi: 10.1016/j.marpolbul.2014.06.001.
7. Courtene-Jones, W, Quinn, B, Gary, SF, Mogg, AOM and Narayanaswamy, BE 2017. Microplastic pollution identified in deep-sea water and ingested by benthic invertebrates in the Rockall Trough, North Atlantic Ocean. *Environ Pollut.* **231**, 271-280, doi: 10.1016/j.envpol.2017.08.026.
8. Galgani, F 2013. Marine litter within the European marine strategy framework directive. *ICES J. Mar. Sci.* **70(6)**, 1055–1064, DOI: <https://doi.org/10.1093/icesjms/fst122>.
9. Browne, MA et al 2011. Accumulation of microplastic on shorelines worldwide: sources and sinks. *Environ. Sci. Technol.* **45(21)**, 9175–9179, doi: 10.1021/es201811s.
10. Shaoliang, Z et al. 2019. Microplastics in the environment: A review of analytical methods, distribution, and biological effects. *TrAC Trends in Analytical Chemistry* **111**, 62-72, <https://doi.org/10.1016/j.trac.2018.12.002>.
11. Myszograj, M 2020. Microplastic in Food and Drinking Water - Environmental Monitoring Data. *Civil and Environmental Engineering Reports* **30(4)**, 201-209, <https://doi.org/10.2478/ceer-2020-0060>.
12. Zhang, K et al 2021. Understanding plastic degradation and microplastic formation in the environment: A review. *Environmental Pollution* **274**, 116554, doi: 10.1016/j.envpol.2021.116554.
13. Fahrenfeld, NL, Arbuckle-Keil, G, Beni, NN, Bartelt-Hunt, SL, Naderi Beni, N and Bartelt-Hunt, SL 2019. Source tracking microplastics in the freshwater environment. *Trends in Analytical Chemistry* **112**, 248-254, doi: <https://doi.org/10.1016/j.trac.2018.11.030>.
14. Fernández-González, V, Andrade-Garda, JM, López-Mahía, P and Muniategui-Lorenzo, S 2021. Impact of weathering on the chemical identification of microplastics

- from usual packaging polymers in the marine environment. *Analytica Chimica Acta* 179-188, doi: 10.1016/j.aca.2020.11.002.
15. Ana, B, Silva, Ana S Bastos, Celine, IL, Justino, João, P da Costa, Armando, C. Duarte and Teresa, AP Rocha-Santos 2018. Microplastics in the environment: Challenges in analytical chemistry - A review. *Analytica Chimica Acta* **2018**, 1017, 1-19, doi: 10.1016/j.aca.2018.02.043.
  16. Browne, MA, Galloway, T and Thompson, R 2007. Microplastic--an emerging contaminant of potential concern? *Integr Environ Assess Manag.* **2007**, 559–561.
  17. Singh, B and Sharma, N 2008. Mechanistic implications of plastic degradation. *Polym Degrad Stab* **2008**, 93, 561–584.
  18. Hisham, AM 2016. Polypropylene as a Promising Plastic: A Review. *American Journal of Polymer Science* **6(1)**,1-11, doi: 10.5923/j.ajps.20160601.01.
  19. Peng, L, Xin, Z, Xiaowei, W, Jinli, L, Hanyu, W and Shixiang, G 2020. Effect of weathering on environmental behavior of microplastics: Properties, sorption and potential risks. *Chemosphere* **242**, 125193, doi: 10.1016/j.chemosphere.2019.125193.
  20. Brandon, J, Goldstein, M and Ohman, MD 2016. Long-term aging and degradation of microplastic particles: comparing in situ oceanic and experimental weathering patterns. *Mar. Pollut. Bull.* **110(1)**, 299-308, doi: 10.1016/j.marpolbul.2016.06.048.
  21. Lenz, R, Enders, K, Stedmon, CA, MacKenzie, DMAA, Gissel Nielsen, T and Nielsen, TG 2015. A critical assessment of visual identification of marine microplastic using Raman spectroscopy for analysis improvement. *Marine Pollution Bulletin* **100(1)**,82-91,doi: <https://doi.org/10.1016/j.marpolbul.2015.09.026>.
  22. Sathish, N, Jeyasanta, I and Patterson, J 2019. Abundance, characteristics and surface degradation features of microplastics in beach sediments of five coastal areas in Tamil Nadu, India. *Marine Pollution Bulletin* **142**,112-118, doi: 10.1016/j.marpolbul.2019.03.037.
  23. Ter Halle, A, Ladirat, L, Martignac, M, Mingotaud, AF, Boyron, O and Perez E 2017. To what extent are microplastics from the open ocean weathered? *Environ Pollut.* **227**, 167-174, doi: 10.1016/j.envpol.2017.04.051
  24. Wiczorek-Ciurowa, K, Barbasz, J and Sikora, T 2014. *Mikroskopia Bliskich oddziaływań.*, Eds.; Politechnika Krakowska, Kraków, Poland, 2014.
  25. Hidalgo-Ruz, V, Gutow, L, Thompson, RC and Thiel, M 2012. Microplastics in the marine environment: a review of the methods used for identification and quantification. *Environmental Science Technology* **46**, 3060–3075, <https://doi.org/10.1021/es2031505>.
  26. Lin, L et. al. 2018. Occurrence and distribution of microplastics in an urban river: A case study in the Pearl River along Guangzhou City, China. *Science of the Total Environment* **644**,375–381, doi: 10.1016/j.scitotenv.2018.06.327.
  27. Guidelines for sampling microplastics on sandy beaches, A Rocha International, Available online: <https://www.arocha.org/wp-content/uploads/2018/01/Microplastic-sampling-protocol.pdf>. (accessed on: 7-05-2021)
  28. Internet Journal of Vibrational Spectroscopy – How FTIR works. Available online: [https://www.mt.com/int/en/home/products/L1\\_AutochemProducts/ReactIR/ftir-](https://www.mt.com/int/en/home/products/L1_AutochemProducts/ReactIR/ftir-)



- spectroscopy.html?cmp=sea\_01010123&SE=GOOGLE&Campaign=MT\_AC\_EN\_ROW&Adgroup=In+Situ+Analysis+-+FTIR+Spectroscopy+-+Exact&bookedkeyword=fourier%20transform%20infrared%20spectroscopy&matchtype=e&adtext=403854681257&placement=&network=s&kclid=\_k\_EAIaIQobChMIxvas76m48AIVB9myCh3oNg44EAAYASAAEgIojfD\_BwE\_k\_&gclid=EAIaIQobChMIxvas76m48AIVB9myCh3oNg44EAAYASAAEgIojfD\_BwE (accessed on: 7-05-2021)
29. Technika FTIR. Available online: <http://mitr.p.lodz.pl/raman/FTIR.pdf> (accessed on: 7-05-2021).
  30. Przewodnik po spektroskopii Raman. Available online: <https://www.bruker.com/pl/products-and-solutions/infrared-and-raman/raman-spectrometers/what-is-raman-spectroscopy.html#:~:text=Spektroskopia%20Raman%20nale%C5%BCy%20do%20kategorii,a%20nast%C4%99pnie%20interpretuj%C4%85c%20t%C4%99%20interkcj%C4%99.> (accessed on: 7-05-2021).
  31. Pethica, JB and Oliver, WC 1987. Tip Surface Interactions in STM and AFM. *Physica Scripta* **T19**, 61-66.
  32. Baykara, MZ and Schwarz, UD 2016. Atomic force microscopy: methods and applications. *Encyclopedia of Spectroscopy and Spectrometry*. 70-75, <http://dx.doi.org/10.1016/B978-0-12-409547-2.12141-9>.
  33. Microscope: BioScope Catalyst, Experiment Description. User guide. Description of experiment selection in the software NanoScope 9.0.
  34. Hummel Polymer and Additives FT-IR Spectral Library. Available online: <https://www.thermofisher.com/order/catalog/product/834-008601#/834-008601>(accessed on: 21-05-2021).
  35. Hooshmand Zaferani, S 2018. *Introduction of polymer-based nanocomposites*. Woodhead Publishing Series in Composites Science and Engineering, Polymer-based Nanocomposites for Energy and Environmental Applications. Jawaid, M., Mansoob, Khan M.; Woodhead Publishing 1-25, ISBN 9780081022627, <https://doi.org/10.1016/B978-0-08-102262-7.00001-5>.
  36. Tosin, M, Weber, M, Siotto, M, Lott, C and Degli-Innocenti, F 2012. Laboratory test methods to determine the degradation of plastics in marine environmental conditions. *Frontiers in Microbiology* **3**,225, doi: 10.3389/fmicb.2012.00225.
  37. Xu et.al 2019. FTIR and Raman imaging for microplastics analysis: State of the art, challenges and prospects. *Trends in Analytical Chemistry* **119**, 115629. doi: 10.1016/j.trac.2019.115629.
  38. The American Society Of Mechanical Engineers. Surface Texture; (Surface Roughness, Waviness, and Lay); ASME B46.1-2009; (Revision of ASME B46.1-2002). NanoScope Analysis – Help in software: Analysis Functions > Roughness > Roughness Parameters.
  39. Stachowiak, GW and Batchelor, AW 2005. *Engineering tribology*. Abrasive, erosive and Cavitation Wear. Third Edition Elsevier.
  40. Ashrafzadeh, H and Ashrafzadeh, F 2012. A numerical 3D simulation for prediction of wear caused by solid particle impact. *Wear* **276-277**, 75-84, <https://doi.org/10.1016/j.wear.2011.12.003>.

41. Hejwowski, T 2013. *Nowoczesne powłoki nakładane cieplnie odporne na zużycie ściernie i erozyjne*. Monografie –Politechnika Lubelska, Lublin.
42. Wang, Z et al. 2018. Sorption behaviors of phenanthrene on the microplastics identified in a mariculture farm in Xiangshan Bay, Southeastern China. *Science of the Total Environment* 1617-1626, doi: 10.1016/j.scitotenv.2018.02.146.
43. Burrows, SD, Frustaci, S, Thomas, KV and Galloway, T 2020. Expanding exploration of dynamic microplastic surface characteristics and interactions. *Trends in Analytical Chemistry* **130**, 115993, <https://doi.org/10.1016/j.trac.2020.115993>.
44. Selvam, S, Manisha, A, Venkatramanan, S, Chung, SY, Paramasivam, CR and Singaraja, C 2020. Microplastic presence in commercial marine sea salts: A baseline study along Tuticorin Coastal salt pan stations, Gulf of Mannar, South India. *Marine Pollution Bulletin* **150**, 110675, doi: 10.1016/j.marpolbul.2019.110675.
45. Warstwa wierzchnia. Chropowatość i falistość powierzchni. Available online: [https://www.pwsz.konin.edu.pl/images/media\\_pliki/file/4554\\_pl\\_7.rozdzial-v.pdf](https://www.pwsz.konin.edu.pl/images/media_pliki/file/4554_pl_7.rozdzial-v.pdf) (accessed on: 24-05-2021).

*Editor received the manuscript: 28.10.2021*